Revealing Long-Term Multi-Factor Climate Impacts on Antarctic Phytoplankton: A Trend-Based Approach Using STL and Piecewise SEM

Hitomi Tanaka[1,*], Hideyuki Doi [1], and Ryosuke Iritani[2]

[1]Graduate School of Informatics, Kyoto University, Kyoto, Japan
[2]RIKEN Center for Interdisciplinary Theoretical and Mathematical Sciences (iTHEMS), Wako, Saitama, Japan
[*]Corresponding author: Hitomi Tanaka (htanaka.ep425@gmail.com)

June 3, 2025

Abstract

Climate change imposes multiple interacting stressors on ocean ecosystems. The Southern Ocean is among the regions where these impacts are particularly pronounced. Phytoplankton, which perform the bulk of primary production, both maintain the Antarctic marine food web and contribute to the role of the Southern Ocean as the largest oceanic sink for atmospheric CO_2. Previous observational and modeling studies have revealed certain drivers–phytoplankton relationships and highlighted the important confounding factors. In this study, we quantified how climate and environmental drivers interact and influence phytoplankton biomass over a 20-year period, across the entire Southern Ocean, within a multi-factor framework. Specifically, we examined the relationships among atmospheric CO_2, surface water pH, sea ice concentration, sea surface temperature, mixed layer depth, dissolved iron concentration, and chlorophyll *a* concentration. To perform this analysis, we introduced and applied two novel methodological approaches. Firstly, to address seasonal autocorrelation, we combined seasonal trend decomposition using LOESS (STL) with piecewise structural equation modeling (SEM). This approach allowed for robust estimation of long-term driver magnitudes and causal pathways, even in the presence of limited sample sizes and complex data structures. Secondly, given the highly interconnected nature of environmental drivers, we employed a data-driven SEM approach to objectively identify causal structures and avoid biases associated with a priori pathway selection. Our results show a clear signal of ocean acidification driven by increasing CO_2, iron limitation of phytoplankton biomass during spring, and seasonal differences in both the magnitude and structure of the causal pathways, demonstrating the dynamic nature of seasonal processes in the Southern Ocean. This study presents the first Southern Ocean-wide, multi-factor assessment of climate and environmental impacts on phytoplankton biomass over a two-decade period. It introduces a methodological framework mitigates seasonal autocorrelation to accurately capture long-term seasonal trends, and demonstrates the utility of data-driven causal discovery in resolving complex ecological interactions.

Keywords: Climate change; CO_2; the Southern Ocean; phytoplankton; stratification; ocean acidification; dissolved iron; nutrient cycle, SST, warming, sea ice melt; trend analysis; causal discovery

1 Introduction

Climate change imposes multiple interacting stressors on ocean ecosystems [1], including warming [2], freshening [3][4], ocean acidification [5], sea-ice loss [6][7], increased water stratification [8], and altered nutrient regimes [9][10], among others. It is necessary to investigate the cumulative impacts of various concurrent stressors on marine systems[11]. The Southern Ocean is the largest oceanic sink for atmospheric CO_2 [12] and is particularly sensitive to the impacts of climate change, including ocean acidification[13] and the melting of ice shelves and sea ice[14]. Given its major role in global carbon cycling and climate regulation, understanding the Southern Ocean's response to these changes is essential for understanding the impact of climate change. Furthermore, the global ocean acts as a major carbon sink, having absorbed approximately 25–30% of anthropogenic CO_2 emissions. Notably, about 40% of this uptake has occurred in the Southern Ocean [15]. Without this oceanic absorption, atmospheric CO_2 concentrations would be roughly 50% higher than current levels [15]. This uptake of CO_2 is partly driven by phytoplankton, which absorb CO_2 through photosynthesis and transport it to the

deep ocean via vertical fluxes [16]. Primary production by Southern Ocean phytoplankton also plays a key role in sustaining biodiversity and fueling the marine food web [17]. Therefore, studying phytoplankton dynamics in the Southern Ocean is essential for understanding the major impacts of climate change.

Recent modeling studies have advanced our understanding of the complex interactions among multiple environmental drivers and their influences on phytoplankton. Kwiatkowski et al.[18] projected simultaneous 21st-century ocean warming, acidification, deoxygenation, and reduced net primary production. Schmittner et al. [19] demonstrated that global nutrient and productivity patterns are highly sensitive to vertical mixing and organic-matter cycling. Fu et al. [20] showed that intensified stratification drives widespread declines in net primary and export production. Nevertheless, most of these studies still investigate some set of drivers, and multivariate assessments that compare the relative importance of several stressors remain scarce (e.g. [21]). Consequently, the approaches capable of identifying dominant factors and emergent interactions across a broader parameter space are still needed.

Here, we leverage two recent advances that make it feasible to assess the long-term, large-spatial scale, and multivariate interactions between climate forcing and ocean environmental variables. First, two decades of reanalysis and observation products (MERRA NOBM, COBE-SST, NSIDC, and others) provide monthly data on atmospheric CO_2, surface water pH, sea ice concentration, sea surface temperature, mixed layer depth of the ocean, dissolved iron concentration and chlorophyll *a* concentration. Second, piecewise structural equation modeling (piecewise SEM) provides a robust framework to assess the relative importance of interacting environmental drivers and identify key causal factors[22][23]. It offers flexibility to accommodate non-normal distributions, temporal autocorrelation, and hierarchical structures commonly present in ecological data, while retaining the capacity to test causal hypotheses[24][23].

Using 240 monthly composites from 1998 to 2017, we ask:

1. Which environmental drivers exert the strongest direct and indirect controls on biomass of phytoplankton in the southern ocean?
2. Do the dominant pathways of the causal relationships among the variables vary seasonally?

By delivering the first basin-wide multivariate path analysis of the Southern Ocean, our study clarifies the long-term, large-spatial scale, and multivariate interactions between climate forcing and ocean environmental variables using the datasets.

However, conducting this analysis required addressing two remaining challenges: removing strong seasonal autocorrelation of the variables and developing a method to determine the underlying causal relationships.

The first challenge, seasonal autocorrelation, arises from the clear 12-month cycle present in the monthly time series (Fig. 1). If not properly accounted for, this seasonal pattern can distort the path coefficients and result in inaccurate conclusions when estimating long-term trends.

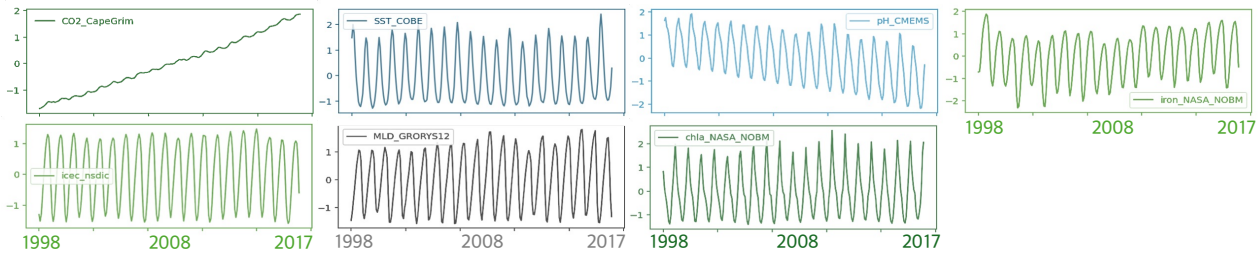

Figure 1: Original Dataset Exhibiting Strong Seasonal Autocorrelation

Accurate estimation of long-term effects requires appropriately handling strong seasonal autocorrelation. If not addressed, this seasonality may affect the stability of path coefficients and lead to misleading conclusions about long-term trends.

Secondary, we face a key question: which path structure most accurately represents the system we aim to understand? SEM is attractive because it tests a hypothesized the network with global fit indices and provides the relative weight of every link [25]. To formulate a hypothesis about the path structure, previous studies have identified many pairwise relationships. For example, CO_2 driven acidification [5][26], the impact of stratification on phytoplankton [9], and the ice albedo feedback that amplifies the warming of the sea surface [27]. Yet these effects form a densely interconnected web: rising CO_2 warms the surface ocean, accelerates ice melt, and further amplifies surface temperatures through feedback processes. These changes influence phytoplankton, which in turn absorb CO_2 through photosynthesis, triggering further interactions within the system.

When the network is this complex, deciding a priori which paths to include can bias the results, and the usual practice of adding or deleting links until the model fits may become arbitrary. Thus, although SEM remains a valid framework, a strictly hypothesis-driven version is impractical here.

Addressing the Two Key Challenges

To overcome the two major challenges, namely seasonal autocorrelation and structural bias, we developed the following approach.

1. Removal of Seasonal Autocorrelation

Accounting for or removing seasonal variation is occasionally done in ecological research when analyzing causal relationships [28][29]. As a method to take seasonality into account, classical seasonal autoregressive moving average models (SARMA) are well suited to capture seasonal dependence [30], but require relatively long records and cannot be embedded within the current implementation of piecewise SEM without substantial modification. Seasonal dummy variables offer a data efficient alternative [31], yet they average conditions within each season and therefore mask gradual, long-term change. Cubic spline or other flexible trend smoothers could, in principle, isolate long-term signals [31], but the resulting mixture of linear and higher-order polynomial terms is not currently compatible with piecewise SEM's estimation engine.

We therefore implement Seasonal and Trend decomposition using Loess (STL) [32] as a preprocessing step. Removing the seasonal component suppresses the strong intra-annual autocorrelation while preserving the deseasonalized trend and anomaly series (Fig. 3). A piecewise SEM can then be fitted to the resulting data, with an AR(1) error structure added to the residuals [31]; this combination enables robust estimation of long-term driver magnitudes and pathways despite limited sample sizes and complex structure of data.

2. Method to Determine the Underlying Structural Relationships without Prior Bias

To limit subjectivity, we conducted a data-driven SEM workflow. Data-driven causal discovery is an emerging tool for structuring the SEM models. Xu et al. [33] proposed a hybrid approach combining Bayesian networks and SEM, where a data-driven causal structure is first learned using a Bayesian network and then refined and validated with SEM, reducing reliance on first assumptions and improving model accuracy and reliability. The Bayesian networks also recover directed acyclic graphs like piecewise SEM[34], but their nonlinear probabilistic links are sometimes not compatible with the linear structure of SEM or piecewise SEM, and also it is difficult to take advantage of piecewise SEM's strengths in handling non-normal data and hierarchical structures.

To address this, we implemented a beam search algorithm to explore candidate models that meet the goodness of fit index of piecewise SEM [24], and then selected the most appropriate model using a combination of information criteria[35][36] and prior ecological knowledge. This approach takes full advantage of the data structures that piecewise SEM can accommodate, while initially minimizing analyst bias by systematically exploring model space using goodness of fit indices and information criteria. At the same time, it allows for the selective incorporation of prior knowledge, achieving a balanced integration of data-driven discovery and expert-informed reasoning.

To clarify the multifaceted influence of increasing atmospheric CO_2 on Antarctic phytoplankton, we first eliminate the pronounced seasonal cycle with STL [32]. We then analyzed the deseasonalized data using piecewise SEM with an AR(1) error term, a setup capable of handling limited sample sizes while accounting for residual autocorrelation [31]. In addition, we conduct a data-driven SEM framework which eliminate analyst bias. Our analyses provide a robust view of the long-term, basin-scale multivariate links among CO_2 forcing, ocean environmental conditions, and phytoplankton dynamics.

2 Method

Data

We used the publicly available datasets as follows and listed in Table 1.

- **Atmospheric CO_2: CSIRO Cape Grim (time: 1976 - present**) [37] - Continuous Southern-Hemisphere background record with minimal urban or volcanic influence.

- **Sea surface temperature: COBE-SST v2 (time: 1850 - present, resolution: 1°)** [38] [39] - The longest 1° observational reconstruction, using an EOF-based statistical reconstruction with updated bucket corrections.
- **Sea ice concentration: NOAA/NSIDC Sea-Ice CDR v5 (1978 - present, 12.5 km)** [40] - Daily and monthly passive-microwave retrieval with cross-sensor calibration.
- **Surface water pH: Copernicus Surface Ocean Carbon Fields (1985 - present, monthly, 0.25°)** [41] [42][43]. - A neural-network reconstruction based on SOCAT ship observations, delivering gap-free global coverage.
- **Mixed-layer depth: Copernicus GLORYS12V1 (1993 - present, 1/12°)** [44][45] - Eddy-resolving physical reanalysis that assimilates T/S profiles, altimeter SSH, SST, and sea-ice. It provides finer resolution than ECCO (0.5°) or GODAS (1°) and supplies the 1990s record absent from Argo-based products.
- **Iron and chlorophyll *a*: NASA MERRA-NOBM (1998 - 2017, monthly, 1.25° × 2/3°)** [46]- One of the few global biogeochemical reanalysis that simultaneously assimilates satellite chlorophyll and outputs iron together with chlorophyll in a fully consistent physical environment. It is the sole continuous, gap-free source for both variables.

These datasets were selected because they (i) provide at least 20 years of continuous data, (ii) minimize global spatial gaps, (iii) maintain internal physical-biogeochemical consistency, and (iv) are distributed through officially maintained portals with ongoing updates.

Table 1: Summary of Datasets Used in This Study

Dataset / Provider	Var.	Spatial	Temporal	Period	Type / Processing
Cape Grim GHG[*1] *CSIRO v2025*	CO_2, CH_4	Point	Mon	1976-present	Obs (in situ)
COBE-SST2[*2] *JMA v2.2*	SST	1°	Mon	1850-present	Obs-recon (EOF)
NSIDC SIC CDR[*3] *NSIDC v5*	SIC	12.5 km	Day/Mon	1978-present	Obs (Bootstrap/NT)
Surf. Ocean C Flds[*4] *CMEMS v3*	pH, fCO_2	1/4 °	Mon	1985-present	Obs-recon (NN)
GLORYS12V1[*5] *CMEMS v1*	T,S,u, v, MLD	1/12°	Day/Mon	1993-present	Reanalysis (3D-VAR)
MERRA-NOBM [*6] *NASA GMAO R2020*	Chl-a, DFe	1.25° × 2/3°	Mon	1998-2017	Reanalysis (OC-Chl assim.)

[*1] Cape Grim Baseline Air Pollution Station [37]; data download: `https://capegrim.csiro.au/`.
[*2] Centennial Observation-Based Estimates of SST v2; data download: `https://psl.noaa.gov/data/gridded/data.cobe2.html` (data provided by the NOAA PSL, Boulder, Colorado, USA).[38] [39]
[*3] NOAA /NSIDC Climate Data Record of Passive Microwave Sea Ice Concentration, Version 5; DOI `https://doi.org/10.7265/RJZB-PF78`. [44][45]
[*4] Copernicus Surface ocean carbon fields, Product ID MULTIOBS_GLO_BIO_CARBON_SURFACE_MYNRT_015_008; DOI `https://doi.org/10.48670/moi-00047` [41] [42][43].
[*5] Copernicus Global Ocean Physics Reanalysis (GLORYS12V1), Product ID: GLOBAL_MULTIYEAR_PHY_001_030; DOI `https://doi.org/10.48670/moi-00021`.
[*6] NASA MERRA-NOBM biogeochemical reanalysis [46]; DOI `https://doi.org/10.5067/PT6TXZKSHBW9`10.5067/PT6TXZKSHBW9.
Abbreviations:
Var.- Variable abbreviation; SST – Sea Surface Temperature; SIC – Sea Ice Concentration; fCO_2 – fugacity of CO_2; T, S – temperature, salinity; u, v – horizontal velocity components; DFe - Dissolved Iron; Chl-a – chlorophyll-*a*; NPP – net primary production; Obs-recon – observation-based reconstruction; EOF – empirical orthogonal functions; NT – NASA Team (sea-ice) algorithm; NN – neural network; 3D-VAR – three-dimensional variational data assimilation; OC-Chl assim. – ocean-color chlorophyll assimilation.

Analytical workflow

The analytical workflow is shown in Fig 2 , and the analysis was conducted through the following steps.

1. **Aggregation and standardization**
For every environmental parameter, the monthly means were calculated for all grid cells located south of the Polar Front (PF), the oceanic front that separates subantarctic water from Antarctic surface water. The south region of PF is known as a High Nutrient, Low Chlorophyll (HNLC) area where primary production is highly sensitive to climate change due to dissolved iron limitation and glacial melting. Since the PF is influenced by ocean currents and varies longitudinally, its position was determined by averaging data[47] from 2002 to 2014 at each longitude. Because a simple arithmetic mean of latitude-longitude gridded

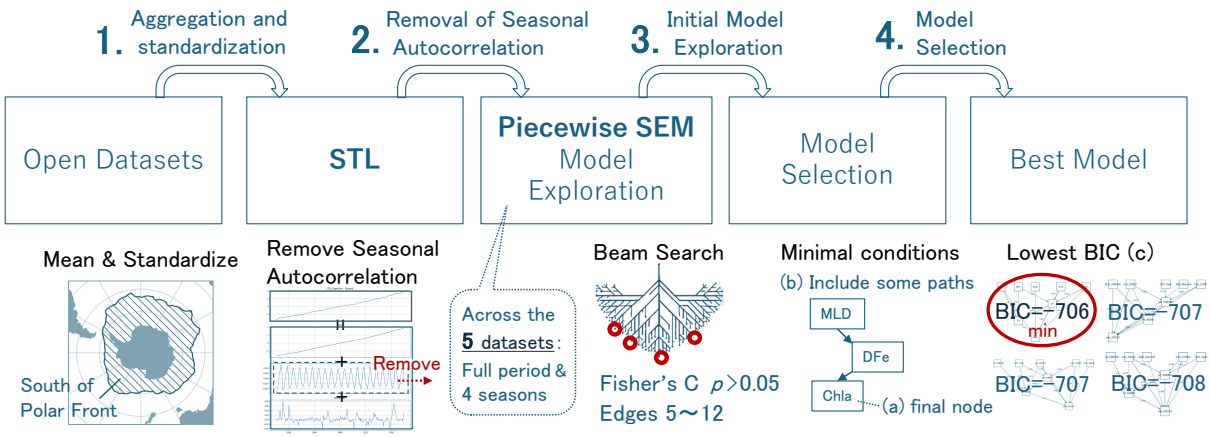

Figure 2: Analytical Workflow

We applied latitude-weighted averaging and standardization to the datasets (1), removed seasonal autocorrelation of the variables using STL decomposition (2), used the beam search to explore the models satisfied the goodness-of-fit indices of piecewise SEM (3), and selected the best model with the lowest BIC after applying minimal conditions (4).

data overrepresents the higher latitudes, we first applied latitude-dependent area weighting and then computed the regional average. Each resulting time series was then standardized with the z-score.

2. **Removal of Seasonal Autocorrelation** (**Fig. 3**, Details are provided in the following section.)
The standardized series were decomposed with Seasonal and Trend decomposition using Loess (STL). We removed the series with the seasonal component. The trend + remainder components are retained for subsequent analyses. Furthermore, after applying STL, the data were divided into seasonal periods: spring (September–November), summer (December–February), autumn (March–May), and winter (June–August). We then conducted the following analysis for five subsets: the full period and each individual season.

3. **Initial Model Exploration**
Using the trend + remainder components series, we explored candidate path models within piecewise SEM framework across the five subsets, including the full period and each four individual season. A beam search algorithm enumerated models which satisfies Fisher's C test ($p_C > 0.05$). The search space was constrained to models containing between 5 and 12 directed edges to limit overfitting and to avoid underfitting. Details on piecewise SEM are provided in the section after next.

4. **Model Selection**
From the set of the models generated during the initial model explorationof piecewise SEM, we applied the minimal additional constraints based on the prior researches to refine the selection — (a) and (b) — and identified the best model accordingly (c). A summary is presented in Table 2.

   (a) We retained only those models in which Chl-*a* appeared exclusively as the terminal node of the partial order. The number of possible path combinations is theoretically estimated at 1.1×10^{18} (for details on the combinatorial calculation, see Fig. S1). For spring and winter, step (b) was skipped, and the analysis proceeded directly to step (c) after applying this condition.

   (b) If the number of candidate models was still too large to manage in (a), each model was required to include three literature supported "white list" pathways.

      (b-1) We included pathways identified in previous studies, such as the effect of increased CO_2 on sea surface temperature ($CO_2 \rightarrow$ SST) and the influence of mixed layer depth on dissolved iron and subsequently on chlorophyll-a concentration (MLD $\rightarrow$ DFe $\rightarrow$ Chl-a). This was applied to the Full Period and autumn analyses. The number of possible path combinations is 1.4×10^{13} (Fig. S1).

      (b-2) For summer, none of the previously identified MLD $\rightarrow$ DFe pathways were detected. Therefore, we included only the $CO_2 \rightarrow$ SST and DFe $\rightarrow$ Chl-a paths from step (b-1). The number of possible path combinations is 2.7×10^{14} (Fig. S1).

(c) From the remaining set, the model with the lowest Baysian Information Criterion (BIC) was chosen as the final model. BIC is a model selection metric that balances model fit and complexity by penalizing the number of parameters, and is designed to consistently select the true model among candidates.

Table 2: Applied Conditions and Number of Candidate Models for Each Season in 4. Model Selection

Season	Model counts from (a)	Applied conditions	Possible combinations	Model counts meeting applied conditions
Spring	25150	(a)	1.1×10^{17}	25150
Summer	968	(a) & (b-2)	2.7×10^{14}	28
Autumn	7385	(a) & (b-1)	1.4×10^{13}	443
Winter	3	(a)	1.1×10^{17}	3
Full Period	9347	(a) & (b-1)	1.4×10^{13}	126

STL and Autocorrelation Reduction

To address seasonal variation, we applied Seasonal and Trend decomposition using Loess (STL) [32]. STL decomposes a time series (Y_t) into three additive components: trend (T_t), seasonal (S_t), and remainder (R_t), as expressed by:

$$Y_t = T_t + S_t + R_t, \tag{1}$$

STL uses LOESS, a local regression technique, to iteratively estimate T_t and S_t in a flexible and robust manner.

After estimating and removing the seasonal component, we obtain a seasonally adjusted series:

$$Y_t^{(\mathrm{adj})} = Y_t - S_t = T_t + R_t. \tag{2}$$

This adjustment is crucial because strong seasonal patterns often introduce significant autocorrelation in the data. By removing S_t, the resulting series $Y_t^{(\mathrm{adj})}$ shows reduced autocorrelation, allowing for more effective modeling and inference based on residual dynamics and trend. Examples of data after STL decomposition are presented in Fig. 3.

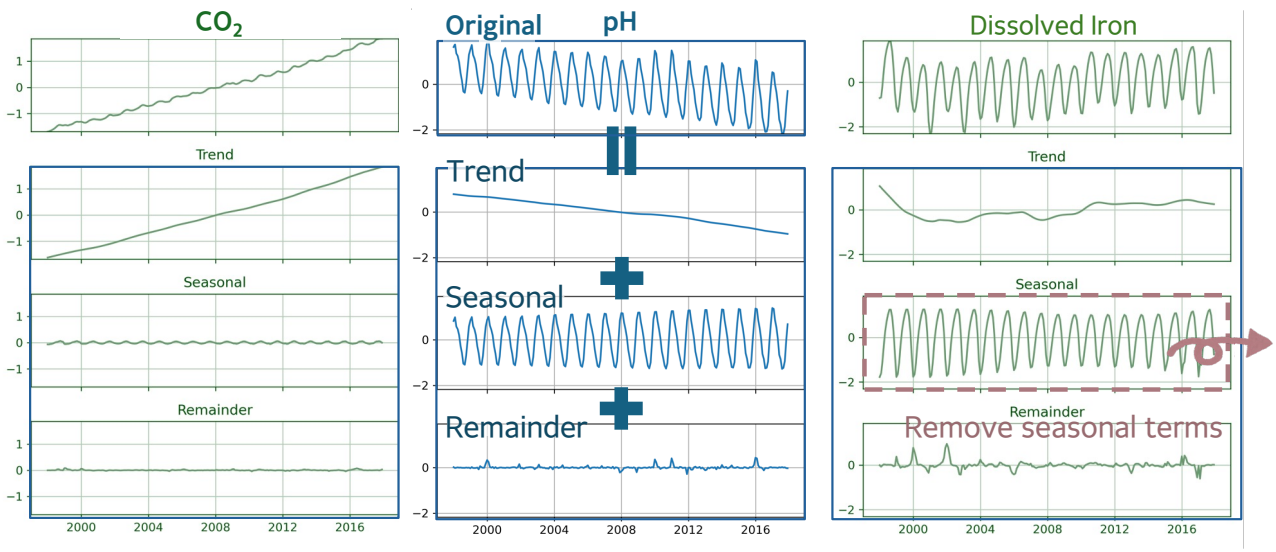

Figure 3: Examples of STL Applied Data

STL is a method separating a time series into seasonal, trend, and remainder components using locally weighted regression. We applied STL to all variables and excluded the seasonal component, thereby facilitating more robust modeling and inference focused on underlying trends and residual variability.

We performed STL using the `statsmodels` package in Python. The Python version used was 3.12.8, and the `statsmodels` [48] version was 0.14.4. The code is shown below.

```python
#import package
  from statsmodels.tsa.seasonal import STL

#STL
  stl = STL(data, period=12, robust=True).fit()
  #The default parameters were: inner_iter=2 / outer_iter=15 / low_pass=13 / trend=23 / seasonal=7
```

The variable `data` refers to the time series data for each climate variable. `period = 12` indicates the periodicity of the sequence, in this case corresponding to 12 months. Setting `robust = TRUE` enables the algorithm to account for outliers. Regarding the default parameters: `inner_iter = 2` ensures greater stability in the separation of seasonal and trend components, though theoretically one iteration is sufficient. `outer_iter = 15` performs 15 rounds of robustness iterations to down-weight outliers; this can be reduced to 10 if outliers are few, to save computation time. `low_pass = 13` is the smallest odd number greater than the period (12), effectively filtering out residual high-frequency noise. `The combination trend = 23` and `seasonal = 7` follows the recommendation of Cleveland [32], and produces a suitably smooth trend component for monthly data.

Piecewise SEM

Piecewise Structural Equation Modeling (SEM) estimates each path as an independent generalized (mixed) model and links them through the rules of graphical d-separation [22]. The results of basis set of conditional independence claims provides a global goodness-of-fit test via Fisher's C statistic [24].

Since parameters are obtained from separate regressions rather than a single covariance matrix, piecewise SEM needs fewer observations than conventional covariance based SEM while still delivering unbiased path coefficients and valid standard errors.

The framework is inherently flexible: any Generalized Linear Model (GLM)/ Linear Mixed Model (LMM)/ Generalized Linear Mixed Model (GLMM) can be inserted into a path, enabling "generalized multilevel path models" that mix link functions, random effects, and distribution families [49] . Temporal or spatial autocorrelation can be handled by specifying residual structures such as AR(1) within each component model.

Thus, piecewise SEM lets the researchers evaluate complex causal networks with modest data and realistic error terms, broadening the applicability of path analysis across disciplines.

We applied Generalized Least Squares (GLS) to the STL and autocorrelation adjusted data $Y_t^{(\mathrm{adj})}$, incorporating an AR(1) structure in the residuals to account for temporal autocorrelation by modeling each month's residual as dependent on the previous month's, thereby capturing the persistence commonly observed in monthly time series data. The model was estimated in `R` using equations such as the following. The `R` version used was 4.4.3, with the `piecewiseSEM` package [49] version 2.3.0.1 and the `nlme` package [50][51] version 3.1-166.

```r
psem(gls(Y3 ~ Y1 + Y2,
        data=data,
        correlation=corAR1(form=~1|full_periods), # for the full period analysis
        #correlation=corAR1(form=~1|individual_year), # for seasonal analysis
        method = "ML"
        ),
      #other formulas
      )
```

Here, `Y1`, `Y2` and `Y3` represent example variables, such as CO_2 and Chl *a*, corresponding to the autocorrelation-adjusted time series $Y_{t,1}^{(\mathrm{adj})}$, $Y_{t,2}^{(\mathrm{adj})}$, $Y_{t,3}^{(\mathrm{adj})}$ introduced in the previous section. The `corAR1` specifies an AR(1) structure in the residuals, applied to the full time series period referred to as the Full Period analysis. While in the seasonal analyses, `corAR1` was applied only within individual years, since, for example, late spring in one year is not temporally correlated with early spring in the following year. The argument `method = "ML"` specifies that model estimation was performed using maximum likelihood (ML), which is required when comparing models using information criteria such as BIC [31].

3 Results

The piecewise-SEM results for the full period and each season are presented in Fig. 4, with global-goodness of fit indices and information criteria summarized in Table 3. The following subsections provide a detailed description of the results for each season and the full-period analysis.

Spring

An increase in CO_2 leads to a decrease in surface water pH, indicating that ocean acidification appears as the most influential pathway. Only in spring, an increase of sea surface temperature results in a decrease in sea ice

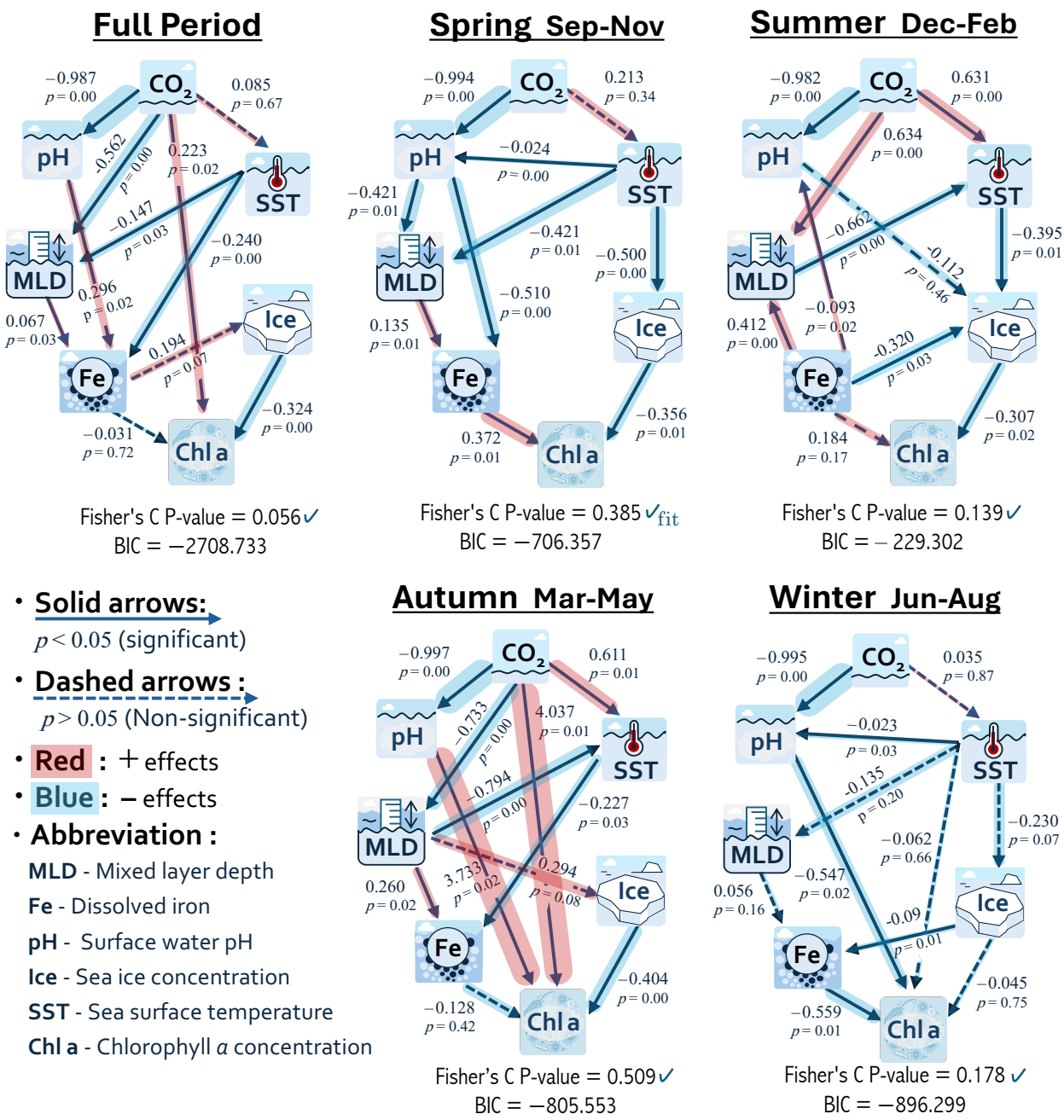

Figure 4: Piecewise SEM Results (R^2) of the Best Models for the Full Period and Individual Seasons

The figures are the results of the best model based on the lowest BIC and validated by Fisher's C test. Solid arrows indicate statistically significant paths ($p < 0.05$) and are the primary focus of interpretation. Red highlights represent the positive effects, blue highlights indicate negative effects, and thicker highlights correspond to larger path coefficients. The figures show both direct and indirect causal relationships among variables; the magnitude of each path coefficient reflects the strength of the relationship.

Table 3: Values of Global Goodness of Fit Indices and Information Criteria

	Global-goodness of fit indices		Information criteria	
Season	Ficher's C	Ficher's C p-value	BIC	AIC
Full Period	30.921	0.056	−2708.733	−2809.672
Spring	23.294	0.385	−706.357	−764.998
Summer	24.498	0.139	−229.302	−347.923
Autumn	19.198	0.509	−805.553	−866.289
Winter	25.636	0.178	−896.299	−957.035

concentration, clearly reflecting the reduction of sea ice due to warming. Furthermore, in spring, higher iron concentrations are associated with increased chlorophyll *a* , suggesting that iron limitation, a characteristic of the Southern Ocean as a high nutrient low chlorophyll (HNLC) region, becomes particularly prominent during this season. There is also a negative relationship between sea ice concentration and chlorophyll *a*, likely because phytoplankton growth is restricted to limited the open water areas during periods of extensive sea ice coverage.

Summer

An increase in CO_2 consistently lowers pH, underscoring ocean acidification as the dominant pathway. The results also show a clear signal of ocean acidification driven by the increase in CO_2 contributes to higher sea surface temperature, and that an increase in SST is associated with a reduction in sea ice extent.

Autumn

In autumn as well, an increase in CO_2 leads to a decrease in pH, indicating that ocean acidification remains the influential pathway. CO_2 is also found to have a direct effect on increasing sea surface temperature.During this season, all parameters show relatively strong effects, with particularly strong relationships observed between CO_2, pH, and chlorophyll *a*.

Winter

In winter as well, an increase in CO_2 leads to a decrease in pH, indicating that ocean acidification remains the most dominant pathway. Compared to the other seasons, the influence of almost all other pathways is relatively weak. This may be attributed to the reduced ocean dynamics during the winter, which limits the expression of the interactions among the variables as distinct pathways.

Full Period and Seasonal Comparisons

Across all seasons, an increasing of CO_2 consistently leads to a decrease in pH, indicating that ocean acidification is a dominant pathway, with path coefficients close to $|1|$. The relationship between deeper mixed layer depth and higher iron concentrations, suggesting the greater nutrient availability, appears clearly in spring, and to a lesser extent when the full period are considered together. Although increasing CO_2 is generally associated with global surface warming through the greenhouse effect, a clear linear relationship between CO_2 and sea surface temperature was observed only in summer and autumn in the Southern Ocean. An increasing of sea surface temperature was associated with a shallower mixed layer depth in both spring and the full period analysis, suggesting the increasing of surface temperature increases stratification. In autumn, the relationship appeared reversed, but overall, a negative correlation between sea surface temperature and mixed layer depth was evident. Furthermore, the path exploration conducted separately for the full period and individual seasons revealed notable differences not only in the magnitude of pathways but also in their structural relationships. These findings highlight that the Southern Ocean exhibits distinct seasonal dynamics.

4 Discussion

In this study, we analyzed the impact of rising atmospheric CO_2 and multiple oceanic drivers on phytoplankton in the Southern Ocean south of the Polar Front, over a 20-year period from 1998 to 2017. With removing seasonal variation of the variables, we firstly applied Seasonal and Trend decomposition using Loess (STL) for piecewise SEM to capture complex relationships among key ecological variables. Using a data-driven approach, we

derived a wide range of insights that extend beyond the explanatory scope of traditional hypothesis-driven SEM.This discussion is structured as follows: we first highlight the key findings, then provide considerations on the methodological approaches employed, and finally present the study's conclusions.

Key Findings

We revealed a range of important findings regarding the biogeochemical and ecological responses of the Southern Ocean to phytoplankton chlorophyll *a*. In the following, we summarize key insights related to ocean acidification, iron limitation , and seasonal differences in these processes.

1. The consistent reduction in pH with increasing CO_2 across all seasons, identifying ocean acidification as the dominant pathway.
   Recent studies have highlighted ongoing ocean acidification in the Southern Ocean. Zemskova et al.[52] showed that dissolved inorganic carbon decreased in the 1990s and 2000s but has increased in surface waters since the 2010s south of 60 Metzl et al. [53] reported a long-term decline in annual mean surface pH from 1985 to 2020 south of the Antarctic Convergence, confirming sustained acidification. This study demonstrates that ocean acidification is not only ongoing but pronounced across the entire Southern Ocean south of the Polar Front over multi-decadal timescales.

2. In spring, elevated iron concentrations correlate with higher chlorophyll *a* levels, indicating that iron limitation in the Southern Ocean is particularly significant during this season.
   Observational studies across the Southern Ocean have consistently shown that iron is a key limiting factor for phytoplankton growth[54] [55] [56]. Satellite data show large blooms near iron sources, and models reveal that iron supply influences plankton composition and export flux—together supporting Martin's iron hypothesis and decades of Southern Ocean research[57]. Our result provides the first large-spactial scale, long-term causal analysis confirming dissolved iron limitation for phytoplankton production across the Southern Ocean, with a novel focus on springtime dynamics using observation, reanalysis data, and path modeling.

3. Distinct seasonal differences were observed in both the magnitude and structure of the causal pathways, demonstrating the dynamic nature of seasonal processes in the Southern Ocean.
   The previous studies have also highlighted various seasonal variations in the Southern Ocean. For example, Tagliabue et al. tagliabue2014surface show that deep water mixing during winter replenishes the mixed layer with iron from subsurface reservoirs. In spring, this iron is rapidly depleted, and summer, vertical iron supply becomes minimal. During this stratified period, phytoplankton increasingly rely on recycled iron, highlighting the importance of internal cycling processes until deep mixing resumes in autumn. Our results also reveal strong seasonal variation in the relationships among mixed layer depth, dissolved iron, and Chl a. However, when viewed over the Full Period, these relationships appear to have a relatively minor overall influence.

While these findings offer valuable insights into oceanic influences on phytoplankton, a more comprehensive understanding would require the inclusion of atmospheric climate variables as well. Our analysis targeted the ocean's response to rising atmospheric CO_2, but other atmospheric forcings still warrant explicit treatment. Variations in stratospheric ozone, aerosol loading, photosynthetically-active radiation (PAR), and the Antarctic Oscillation jointly reshape UV exposure [58], winds, and nutrient supply [59], and could therefore alter the pathways we resolved. Integrating these drivers into future structural models will be essential for a complete causal picture. Also, our analysis integrated datasets from multiple sources, each with its own uncertainty characteristics. While we selected variables known to perform reliably in polar regions, uncertainties remain. Continued data collection and reanalysis of biogeochemical fields will help reduce these uncertainties and are expected to further advance understanding of the Southern Ocean system.

Considerations on the Methodological Approach Adopted in This Study

To remove seasonal autocorrelation, we applied STL [32] to remove seasonal effects, enabling piecewise SEM analysis with an AR(1) residual structure [31]. This approach allows us the reliable estimation of long-term driver effects and causal pathways, with limited sample sizes and complex data structures. Although the previous ecological studies have used deseasonalized residuals or anomalies for statistical analyses (e.g., [28] [29]), and the others have incorporated seasonal indices directly into SEMs (e.g. [60]), To our knowledge, there are no evidence of STL-filtered data being directly used in SEM or piecewise SEM. Our approach with removing seasonal components via STL and analyzing the resulting trend and anomalies with piecewise SEM, offers a

novel contribution, particularly in long-term dataset with seasonal dynamics,where such applications remain largely unexplored.

As for data-driven SEM, we applied a beam search strategy to identify the candidate models that satisfy the goodness-of-fit requirements of piecewise SEM, and subsequently refined model selection by integrating information theoretic metrics with relevant ecological insights. Data-driven causal discovery is emerging as a promising alternative to traditional correlation analysis [33][61], allowing the data itself, rather than relying on prior assumptions, to identify the most plausible pathways. However, its application to Southern Ocean phytoplankton remains unexplored, making this a novel approach in the context of this study. Our data-driven method leverages the flexibility of piecewise SEM to handle complex data structures, while reducing analyst bias in the early stages by using a systematic search based on fit statistics and information-theoretic criteria. It also enables the targeted use of prior ecological knowledge, offering a balanced framework that combines data-driven exploration with theoretical grounding. While traditional research typically tests predefined hypotheses, in this study, we take a data-driven approach that integrates empirical patterns with theoretical insights to uncover underlying causal structures. The data-driven SEM method is powerful in extracting information beyond what hypothesis-driven models can offer, but its flexibility also requires careful handling to avoid subjective bias. The model space under our constraints included at least 10^{13} possible structures(see S1 4.), indicating the data-driven foundation of the approach. Importantly, to generalize this method, future research must establish transparent reporting standards, including the size of the model space, the number of models evaluated, and the rationale for constraints, and promote reproducibility through open data and clear workflows.

Conclusion

This study conducted a comprehensive, multi-factor structural analysis of phytoplankton biomass in the Southern Ocean and key ocean environmental variables using an unprecedented 20-year record (1998–2017) spanning the entire Southern Ocean south of the Polar Front. We identified a clear signal of ocean acidification driven by the increasing of CO_2, persistent iron limitation of phytoplankton, and a pronounced intensification of this iron stress during spring. We also found that the strength and even the direction of many relationships varies markedly with season. To analyze the long-term impacts of complex drivers with strong seasonal autocorrelation, we developed a novel framework combining STL with piecewise SEM. By applying SEM in a data-driven way and interpreting the results alongside existing knowledge, we were able to uncover new insights into the impact of increasing CO_2 and multiple oceanic drivers on phytoplankton in the Southern Ocean. While this study focused on atmospheric CO_2 and oceanic variables to phytoplankton biomass, future work can incorporate broader climate drivers, such as stratospheric ozone, the Antarctic Oscillation, aerosols, and photosynthetically active radiation. Including these factors will help build a more integrated causal picture of the Southern Ocean system.

Acknowledgements

This study was conducted using the datasets (i) Cape Grim Greenhouse Gas Monitoring Data v2025-02 (CSIRO Environment & Australian Bureau of Meteorology); (ii) Surface Ocean Carbon Fields (DOI `10.48670/moi-00047`) and (iii) Global Ocean Physics Reanalysis (DOI `10.48670/moi-00021`) as EU Copernicus Marine Service; (iv) NASA GMAO MERRA-NOBM monthly reanalysis R2020; (v) NOAA/NSIDC passive-microwave sea-ice concentration CDR v5 (DOI `10.7265/rjzb-pf78`); and (vi) COBE-SST2 SST & sea-ice v2 (data provided by the NOAA PSL, Boulder, Colorado, USA, from their website at (`https://psl.noaa.gov`). CSIRO and the Australian Bureau of Meteorology make no warranty, expressed or implied, regarding the Cape Grim data. The authors thank JSPS KAKENHI for funding (22K18429 and 22K12461 to HD; 24H01528 and 24H02291 to RI).

References

[1] Ove Hoegh-Guldberg and John F Bruno. The impact of climate change on the world's marine ecosystems. *Science*, 328(5985):1523–1528, 2010. Publisher: American Association for the Advancement of Science.

[2] Andrew J Constable, Jessica Melbourne-Thomas, Stuart P Corney, Kevin R Arrigo, Christophe Barbraud, David KA Barnes, Nathaniel L Bindoff, Philip W Boyd, Angelika Brandt, Daniel P Costa, and others. Climate change and Southern Ocean ecosystems I: how changes in physical habitats directly affect marine biota. *Global change biology*, 20(10):3004–3025, 2014. Publisher: Wiley Online Library.

[3] Ralph F Keeling, Arne Körtzinger, and Nicolas Gruber. Ocean deoxygenation in a warming world. *Annual review of marine science*, 2(1):199–229, 2010. Publisher: Annual Reviews.

[4] Katherina Petrou, Sven A Kranz, Scarlett Trimborn, Christel S Hassler, Sonia Blanco Ameijeiras, Olivia Sackett, Peter J Ralph, and Andrew T Davidson. Southern Ocean phytoplankton physiology in a changing climate. *Journal of Plant Physiology*, 203:135–150, 2016. Publisher: Elsevier.

[5] James C Orr, Victoria J Fabry, Olivier Aumont, Laurent Bopp, Scott C Doney, Richard A Feely, Anand Gnanadesikan, Nicolas Gruber, Akio Ishida, Fortunat Joos, and others. Anthropogenic ocean acidification over the twenty-first century and its impact on calcifying organisms. *Nature*, 437(7059):681–686, 2005. Publisher: Nature Publishing Group UK London.

[6] IPCC. The Ocean and Cryosphere in a Changing Climate Special Report of the Intergovernmental Panel on Climate Change. Technical report, IPCC, 2022.

[7] Kevin R Arrigo and David N Thomas. Large scale importance of sea ice biology in the Southern Ocean. *Antarctic Science*, 16(4):471–486, 2004. Publisher: Cambridge University Press.

[8] Guancheng Li, Lijing Cheng, Jiang Zhu, Kevin E Trenberth, Michael E Mann, and John P Abraham. Increasing ocean stratification over the past half-century. *Nature Climate Change*, 10(12):1116–1123, 2020. Publisher: Nature Publishing Group UK London.

[9] Monika Winder and Ulrich Sommer. Phytoplankton response to a changing climate. *Hydrobiologia*, 698:5–16, 2012. Publisher: Springer.

[10] Jorge L Sarmiento, R Slater, R Barber, L Bopp, SC Doney, AC Hirst, J Kleypas, R Matear, Uwe Mikolajewicz, P Monfray, and others. Response of ocean ecosystems to climate warming. *Global Biogeochemical Cycles*, 18(3), 2004. Publisher: Wiley Online Library.

[11] Julian Gutt, Nancy Bertler, Thomas J Bracegirdle, Alexander Buschmann, Josefino Comiso, Graham Hosie, Enrique Isla, Irene R Schloss, Craig R Smith, Jean Tournadre, and others. The Southern Ocean ecosystem under multiple climate change stresses-an integrated circumpolar assessment. *Global Change Biology*, 21(4):1434–1453, 2015. Publisher: Wiley Online Library.

[12] Thomas L Frölicher, Jorge L Sarmiento, David J Paynter, John P Dunne, John P Krasting, and Michael Winton. Dominance of the Southern Ocean in anthropogenic carbon and heat uptake in CMIP5 models. *Journal of Climate*, 28(2):862–886, 2015. Publisher: American Meteorological Society.

[13] Alyce M Hancock, Andrew T Davidson, John McKinlay, Andrew McMinn, Kai G Schulz, and Rick L van den Enden. Ocean acidification changes the structure of an Antarctic coastal protistan community. *Biogeosciences*, 15(8):2393–2410, 2018. Publisher: Copernicus Publications Göttingen, Germany.

[14] Richard Bintanja, Geert Jan van Oldenborgh, SS Drijfhout, Bert Wouters, and CA Katsman. Important role for ocean warming and increased ice-shelf melt in Antarctic sea-ice expansion. *Nature Geoscience*, 6(5):376–379, 2013. Publisher: Nature Publishing Group UK London.

[15] Stacy L Deppeler and Andrew T Davidson. Southern Ocean phytoplankton in a changing climate. *Frontiers in Marine Science*, 4:40, 2017. Publisher: Frontiers Media SA.

[16] Sandy J. Thomalla, Sarah-Anne Nicholson, Thomas J. Ryan-Keogh, and Marié E. Smith. Widespread changes in Southern Ocean phytoplankton blooms linked to climate drivers. *Nature Climate Change*, 13(9):975–984, September 2023. Publisher: Nature Publishing Group.

[17] Kristen M. Krumhardt, Matthew C. Long, Zephyr T. Sylvester, and Colleen M. Petrik. Climate drivers of Southern Ocean phytoplankton community composition and potential impacts on higher trophic levels. *Frontiers in Marine Science*, 9, August 2022. Publisher: Frontiers.

[18] Lester Kwiatkowski, Olivier Torres, Laurent Bopp, Olivier Aumont, Matthew Chamberlain, James R Christian, John P Dunne, Marion Gehlen, Tatiana Ilyina, Jasmin G John, and others. Twenty-first century ocean warming, acidification, deoxygenation, and upper-ocean nutrient and primary production decline from CMIP6 model projections. *Biogeosciences*, 17(13):3439–3470, 2020. Publisher: Copernicus GmbH.

[19] Andreas Schmittner, Andreas Oschlies, Xavier Giraud, Michael Eby, and Harper L Simmons. A global model of the marine ecosystem for long-term simulations: Sensitivity to ocean mixing, buoyancy forcing, particle sinking, and dissolved organic matter cycling. *Global Biogeochemical Cycles*, 19(3), 2005. Publisher: Wiley Online Library.

[20] Weiwei Fu, James T Randerson, and J Keith Moore. Climate change impacts on net primary production (NPP) and export production (EP) regulated by increasing stratification and phytoplankton community structure in the CMIP5 models. *Biogeosciences*, 13(18):5151–5170, 2016. Publisher: Copernicus GmbH.

[21] Anna F Mosby and Walker O Smith. Structural equation modeling of the influence of environmental factors on summer phytoplankton growth in the Ross Sea. *Polar Biology*, 40:291–299, 2017. Publisher: Springer.

[22] Bill Shipley. A New Inferential Test for Path Models Based on Directed Acyclic Graphs. *Structural Equation Modeling: A Multidisciplinary Journal*, 7(2):206–218, 2000. Publisher: Routledge _eprint: https://doi.org/10.1207/S15328007SEM0702_4.

[23] Bill Shipley. *Cause and Correlation in Biology: A User's Guide to Path Analysis, Structural Equations and Causal Inference with R*. Cambridge University Press, Cambridge, 2 edition, 2016.

[24] Bill Shipley. Confirmatory path analysis in a generalized multilevel context. *Ecology*, 90(2):363–368, 2009. _eprint: https://onlinelibrary.wiley.com/doi/pdf/10.1890/08-1034.1.

[25] James B. Grace. Structural Equation Modeling for Observational Studies. *The Journal of Wildlife Management*, 72(1):14–22, 2008. _eprint: https://onlinelibrary.wiley.com/doi/pdf/10.2193/2007-307.

[26] Blanca Figuerola, Alyce M Hancock, Narissa Bax, Vonda J Cummings, Rachel Downey, Huw J Griffiths, Jodie Smith, and Jonathan S Stark. A review and meta-analysis of potential impacts of ocean acidification on marine calcifiers from the Southern Ocean. *Frontiers in Marine Science*, 8:584445, 2021. Publisher: Frontiers.

[27] Judith A Curry, Julie L Schramm, and Elizabeth E Ebert. Sea ice-albedo climate feedback mechanism. *Journal of Climate*, 8(2):240–247, 1995. Publisher: American Meteorological Society.

[28] Mike Brett. Effects of climatic variability on the thermal properties of Lake Washington. *Limnology and Oceanography*, January 2004.

[29] Craig A. Stow, YoonKyung Cha, Laura T. Johnson, Remegio Confesor, and R. Peter Richards. Long-Term and Seasonal Trend Decomposition of Maumee River Nutrient Inputs to Western Lake Erie. *Environmental Science & Technology*, 49(6):3392–3400, March 2015.

[30] George E. P. Box, Gwilym M. Jenkins, Gregory C. Reinsel, and Greta M. Ljung. Time Series Analysis: Forecasting and Control, 5th Edition | Wiley, 2015.

[31] Alain F. Zuur, Elena N. Ieno, Neil Walker, Anatoly A. Saveliev, and Graham M. Smith. *Mixed effects models and extensions in ecology with R*. Statistics for Biology and Health. Springer, New York, NY, 2009.

[32] Robert B. Cleveland, William S. Cleveland, Jean E. McRae, and Irma Terpenning. STL: a seasonal-trend decomposition procedure based on loess. *Journal of Official Statistics*, 6:3–73, 1990.

[33] Xiao-fu Xu, Jian Sun, Hong-tao Nie, De-kui Yuan, and Jian-hua Tao. Linking structural equation modeling with Bayesian network and its application to coastal phytoplankton dynamics in the Bohai Bay. *China Ocean Engineering*, 30(5):733–748, October 2016.

[34] Judea Pearl. Bayesian networks: A model of self-activated memory for evidential reasoning. In *Proceedings of the 7th conference of the Cognitive Science Society, University of California, Irvine, CA, USA*, pages 15–17, 1985.

[35] Gideon Schwarz. Estimating the dimension of a model. *The annals of statistics*, pages 461–464, 1978. Publisher: JSTOR.

[36] Hirotugu Akaike. Factor Analysis and AIC. *Psychometrika*, 52(3):317–332, September 1987.

[37] CSIRO Environment and Australian Bureau of Meteorology. Cape Grim Greenhouse Gas Monitoring Data. `https://capegrim.csiro.au/`, may 2025. Accessed 2025-02-03.

[38] Japan Meteorological Agency and NOAA Physical Sciences Laboratory. COBE-SST2 Sea Surface Temperature and Sea Ice. `https://psl.noaa.gov/data/gridded/data.cobe2.html`. Data provided by the NOAA PSL, Boulder, Colorado, USA. Accessed 2024-11-16.

[39] Shoji Hirahara, Masayoshi Ishii, and Yoshikazu Fukuda. Centennial-scale sea surface temperature analysis and its uncertainty. *Journal of Climate*, 27:57–75, 2014.

[40] Walt Meier, Florence Fetterer, Ann Windnagel, James Scott Stewart, and Trey Stafford. NOAA/NSIDC Climate Data Record of Passive Microwave Sea Ice Concentration, Version 5, 2024.

[41] Thi Tuyet Trang Chau, Marion Gehlen, and Frédéric Chevallier. A seamless ensemble-based reconstruction of surface ocean pCO_2 and air–sea CO_2 fluxes over the global coastal and open oceans. *Biogeosciences*, 19(4):1087–1109, February 2022. Publisher: Copernicus GmbH.

[42] Thi-Tuyet-Trang Chau, Frédéric Chevallier, and Marion Gehlen. Global Analysis of Surface Ocean CO2 Fugacity and Air-Sea Fluxes With Low Latency. *Geophysical Research Letters*, 51(8):e2023GL106670, 2024. _eprint: https://onlinelibrary.wiley.com/doi/pdf/10.1029/2023GL106670.

[43] Thi-Tuyet-Trang Chau, Marion Gehlen, Nicolas Metzl, and Frédéric Chevallier. CMEMS-LSCE: a global, 0.25°, monthly reconstruction of the surface ocean carbonate system. *Earth System Science Data*, 16(1):121–160, January 2024. Publisher: Copernicus GmbH.

[44] EU Copernicus Marine Service. Global Ocean Physics Reanalysis, 2024. Accessed 2025-02-06.

[45] Jean-Michel Lellouche et al. The copernicus global 1/12° oceanic and sea ice glorys12 reanalysis. *Frontiers in Earth Science*, 9:698876, 2021.

[46] NASA Global Modeling and Assimilation Office (GMAO). MERRA-NOBM (nasa ocean biogeochemical model) reanalysis monthly data.

[47] Natalie M. Freeman and Nicole S. Lovenduski. Mapping the Antarctic Polar Front: weekly realizations from 2002 to 2014. *Earth System Science Data*, 8(1):191–198, May 2016. Publisher: Copernicus GmbH.

[48] Skipper Seabold and Josef Perktold. statsmodels: Econometric and statistical modeling with python. In *9th Python in Science Conference*, 2010.

[49] Jonathan S Lefcheck. piecewiseSEM: Piecewise structural equation modelling in r for ecology, evolution, and systematics. *Methods in Ecology and Evolution*, 7(5):573–579, 2016. Publisher: Wiley Online Library.

[50] José Pinheiro, Douglas Bates, and R Core Team. *nlme: Linear and Nonlinear Mixed Effects Models*, 2025. R package version 3.1-168.

[51] José C. Pinheiro and Douglas M. Bates. *Mixed-Effects Models in S and S-PLUS*. Springer, New York, 2000.

[52] Varvara E. Zemskova, Tai-Long He, Zirui Wan, and Nicolas Grisouard. A deep-learning estimate of the decadal trends in the Southern Ocean carbon storage. *Nature Communications*, 13(1):4056, July 2022. Publisher: Nature Publishing Group.

[53] Nicolas Metzl, Claire Lo Monaco, Coraline Leseurre, Céline Ridame, Gilles Reverdin, Thi Tuyet Trang Chau, Frédéric Chevallier, and Marion Gehlen. Anthropogenic CO_2, air–sea CO_2 fluxes, and acidification in the Southern Ocean: results from a time-series analysis at station OISO-KERFIX (51° S–68° E). *Ocean Science*, 20(3):725–758, June 2024. Publisher: Copernicus GmbH.

[54] Hein J. W. de Baar, Jeroen T. M. de Jong, Dorothée C. E. Bakker, Bettina M. Löscher, Cornelis Veth, Uli Bathmann, and Victor Smetacek. Importance of iron for plankton blooms and carbon dioxide drawdown in the Southern Ocean. *Nature*, 373(6513):412–415, February 1995. Publisher: Nature Publishing Group.

[55] Frank Gervais, Ulf Riebesell, and Maxim Y. Gorbunov. Changes in primary productivity and chlorophyll a in response to iron fertilization in the Southern Polar Frontal Zone. *Limnology and Oceanography*, 47(5):1324–1335, 2002. _eprint: https://onlinelibrary.wiley.com/doi/pdf/10.4319/lo.2002.47.5.1324.

[56] Erin M. Bertrand, Mak A. Saito, Peter A. Lee, Robert B. Dunbar, Peter N. Sedwick, and Giacomo R. Ditullio. Iron limitation of a springtime bacterial and phytoplankton community in the ross sea: implications for vitamin b(12) nutrition. *Frontiers in Microbiology*, 2:160, 2011.

[57] Emma Bazzani, Chiara Lauritano, and Maria Saggiomo. Southern ocean iron limitation of primary production between past knowledge and future projections. *Journal of Marine Science and Engineering*, 11(2):272, 2023. Publisher: MDPI.

[58] Yusuf A Bhatti, Laura E Revell, and Adrian J McDonald. Influences of Antarctic ozone depletion on southern ocean aerosols. *Journal of Geophysical Research: Atmospheres*, 127(18):e2022JD037199, 2022. Publisher: Wiley Online Library.

[59] Jae-Seung Yoon, Keyhong Park, Jisoo Park, Taewook Park, and Tae-Wook Kim. Lagged effect of Southern Annular Mode on chlorophyll-a in the mid-latitude South Pacific and Indian Oceans. *Environmental Research Letters*, 19(4):044032, 2024. Publisher: IOP Publishing.

[60] Matthew G. Slocum and Steve L. Orzell. A Structural Equation Model Analysis of Relationships among ENSO, Seasonal Descriptors and Wildfires. *PLOS ONE*, 8(9):e75946, September 2013. Publisher: Public Library of Science.

[61] Enrico Premi, Mario Grassi, Stefano Gazzina, Barbara Paghera, Daniele Pepe, Silvana Archetti, Alessandro Padovani, and Barbara Borroni. The Neuroimaging Signature of Frontotemporal Lobar Degeneration Associated with Granulin Mutations: An Effective Connectivity Study. *Journal of Nuclear Medicine*, July 2013. Publisher: Society of Nuclear Medicine Section: Basic Science Investigation.

Supplementary Material

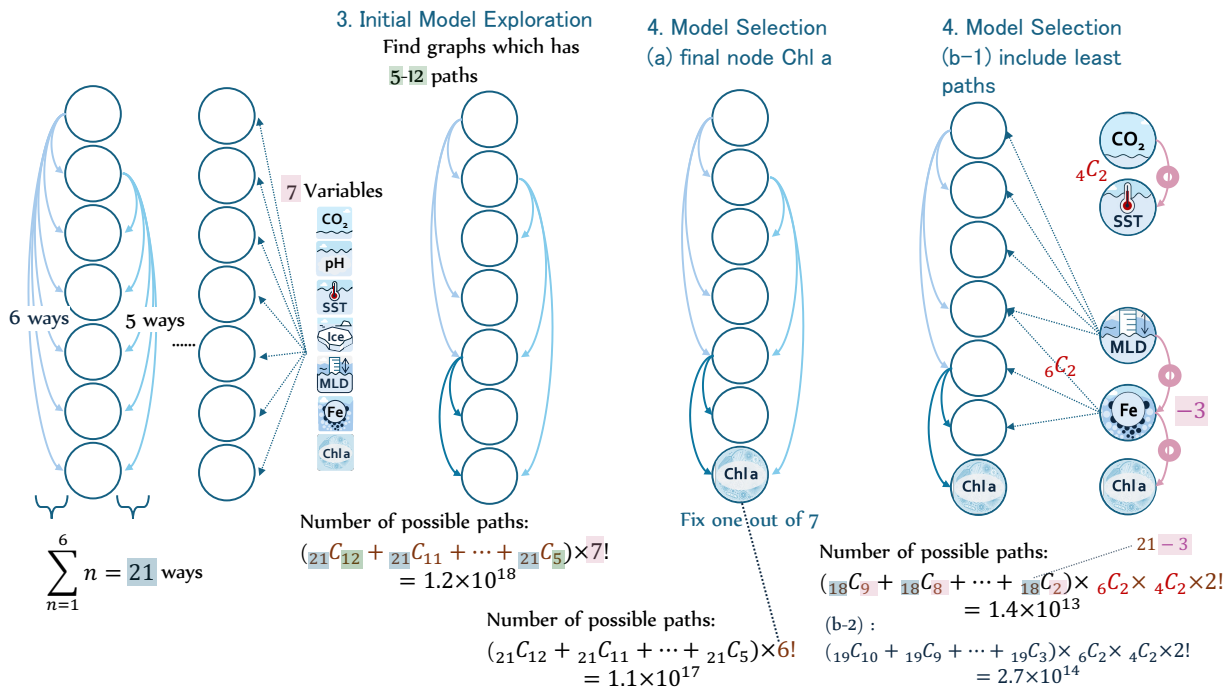

Figure S1: Number of possible paths